Nuclear fragmentation in interactions of 3.7*A* GeV ^{24}Mg projectiles with emulsion targets

M. A. Jilany
Physics Department, Faculty of Science (Sohag), South Valley University, Sohag, Egypt
(Received 10 September 2003; revised manuscript received 29 April 2004; published 9 July 2004)

The process of nuclear fragmentation in interactions of 3.7*A* GeV ^{24}Mg nuclei with the different target nuclei in a nuclear emulsion have been investigated. The total charge distributions of nuclear fragments are well described by the predictions of the extended Glauber model. The multiplicity and charge distributions of fragments with $Z \geqslant 5$ in quasinucleon target events are found to agree satisfactorily with the calculations of the bond percolation model. The fragmentation of the projectile nucleus depends strongly on the target mass. The probability of interactions without any projectile fragments with charges $Z > 2$ is zero for a hydrogen target, but increases by increasing the mass of the target. The disruption of a projectile nucleus is more severe in interactions with the heavy target nuclei than with the light ones. The topology for the nuclear fragmentation channels in interactions of the different projectiles with the different components of emulsion nuclei in the energy range 3.7–200*A* GeV was analyzed. The average multiplicities and the relative rates of nuclear fragmentation channels from the incident nuclei are almost the same for all projectiles at different energies, revealing that the modes of nuclear fragmentation are energy independent. The stripped processes with relativistic hydrogen and/or helium fragments are the dominant in all projectiles. Helium fragments are the most frequent among the multiple charged fragments and the fractional yield of nuclear fragmentation channels without projectile fragments heavier than helium fragments is about 27% of the total sample. The interactions in which the projectile nuclei break up into single charged particles only represent ≈14% of the total sample and are mostly due to central collisions in which the majority of projectile nucleons have participated in the first stage of the collisions.

DOI: 10.1103/PhysRevC.70.014901 PACS number(s): 29.40.Rg, 25.75.−q

I. INTRODUCTION

Nuclear fragmentation and its possible connection with a critical phenomenon or a phase transition has been the subject of intensive theoretical and experimental investigations in the interactions of relativistic heavy nuclei. These studies can provide information about the fragmentation mechanism and liquid-gas phase transition process in hot nuclei and help to trace the reaction mechanism of nucleus-nucleus interactions [1–4]. According to the participant-spectator model [5–7], the overlapping region of nuclear volumes of two colliding nuclei is called the participant part where multiple production of new particles occur and the nuclear matter breaks up into nucleons. This process is the first stage of the collision, which is very rapid having a short time almost equivalent to the time taken by light to cross the target nucleus. The remaining parts of nuclei that do not participate in the disintegration process are called the spectator regions of projectile and target nuclei. During this production process, a fraction of available energy is transferred to the spectator parts of colliding nuclei, leaving those nuclear remnants in an excited state. After this stage, the deexcitation of the nuclear remnants takes place. The latter process, called nuclear fragmentation, particularly the fragmentation of the relativistic projectile nucleus, is interesting in this research. The fragmentation of a heavy projectile leads to the emission of fragments with a broad mass spectrum which extends from the lightest fragments, i.e., nucleons, to the fragments as heavy as the disintegrating projectile. This broad mass range is correlated with the large range of fragment multiplicities. Thus one observes a large diversity of fragmentation modes, which may correspond to different breakup mechanisms: from emission of a single heavy fragment or through binary fission to a complete breakup into nucleons [8–11].

The spectator fragments of the projectile nucleus have momentum per nucleon almost equal to that of the parent nucleus, so they are essentially emitted inside a narrow forward-angular cone centered around the direction of the incident beam, and remain relativistic. Hence, unlike the fragments of the target nucleus, the heavy fragments of the projectile nucleus are very easily and reliably distinguished from all other particles emitted from the collision vertex [12].

The emulsion technique allows studies of produced charged particles and their distributions in space are with higher accuracy and a larger acceptance than most of the current counter experiments, although with rather limited statistics. A great advantage of emulsions is that the same projectile-target system can be studied at different available energies with identical detectors and with identical analysis criteria [13–16]. However, one of the main problems encountered in interpreting the results from nuclear emulsion experiments is the nonhomogeneous composition of the emulsion, which basically consists of three groups of nuclei: hydrogen, light (carbon, nitrogen, oxygen), and heavy (bromine, silver). The separation of a minimum bias sample of ^{24}Mg interactions with the three main groups of target nuclei allowed us to make simultaneous analyses of fragmentation processes of the projectile and the target nuclei as well as studying the production processes as a function of the target mass, taking full advantage of the nuclear emulsion technique [14,15].

TABLE I. The statistics of events in interactions of ^{24}Mg, ^{28}Si, and ^{32}S projectiles with the various components of target emulsion nuclei at different energies.

Projectile	^{24}Mg	^{28}Si		^{32}S
Energy (A GeV)	3.7	3.7	14.6	200
Total number of collisions	1025	1986	955	775
$n_h=0,1$	211	443	265	283
$n_h=2-7$	364	734	328	234
$n_h\geqslant 8$	450	809	362	258
$N(2\leqslant n_h\leqslant 7)/N(n_h\geqslant 8)$	0.81 ± 0.08	0.91 ± 0.07	0.91 ± 0.09	0.91 ± 0.12
Events with the total destruction of the projectile nucleus with ($Z\leqslant 2$)				
$n_h=0,1$	38	75	58	50
$n_h=2-7$	153	265	135	80
$n_h\geqslant 8$	330	557	273	166
$N(2\leqslant n_h\leqslant 7)/N(n_h\geqslant 8)$	0.46 ± 0.06	0.48 ± 0.05	0.49 ± 0.07	0.48 ± 0.09
Reference	present work	[26]	[26]	[26]

Competing models suggest different decay mechanisms and experiments have yet to discriminate between several theoretical scenarios that ranged from the sequential decay of the compound nucleus [17,18] to statistical nuclear models [19,20] and percolation models [21–23]. The percolation models predicted a power law distribution in fragment sizes near the critical point [21,22]. These models still enjoy great popularity and have been employed in the analysis of Au multifragmentation data obtained by the EOS Collaboration [24,25].

The aim of the present paper is to investigate the breakup of relativistic ^{24}Mg nuclei during interactions with the different target nuclei in nuclear emulsion (Em) at 3.7A GeV. The experimental data for different charges of relativistic nuclei that emerge in the incident ^{24}Mg projectile on emulsion targets are compared with the predictions of the two theoretical models. The topological structure of ^{24}Mg nuclear fragments is studied and compared with those obtained by Adamovich *et al.* [26] in interactions of 3.7A GeV ^{28}Si, 14.6A GeV ^{28}S, and 200A GeV ^{32}S projectiles with the target emulsion nuclei.

II. EXPERIMENTAL DETAILS

The experimental data have been obtained from nuclear track emulsion, which was used as a target. The stack was composed of BR-2 nuclear emulsion pellicles with dimensions of 10×20 cm^2 and 600 μm thick was exposed horizontally to ^{24}Mg ions with energy 3.7A GeV at the DUBNA Synchrophasotron. The sensitivity of emulsion was about 30 grains per unit length of 100 μm for singly charged particles with minimal ionization. Primary interactions were found along-the-track double scanning (fast in the forward and slow in the backward) of the processed emulsion plates under high magnification. A total of 1025 inelastic interactions of ^{24}Mg projectile with emulsion nuclei were picked up by along 98.50 m of primary track length, leading to a mean free path of 9.61 ± 0.30 cm, which correspond to a total inelastic cross section of 1335 ± 42 mb. The present measured values of ^{24}Mg in emulsion are in systematic agreement with those measured previously for different systems [27,28], reflecting the high efficiency of scanning. The scanning details, the classifications of charged secondary tracks, and the projectile fragments were presented previously [28].

In each event, $Z_{\max}$ is the maximum possible charge of a given projectile fragment. The total stripped charge of the projectile fragments Q is defined as $Q=\Sigma_i n_i Z_i$, where n_i is the number of projectile fragments with charge $Z_i\geqslant 1$ and the summation is carried out over all such fragments in an event. The numbers of fast singly charged fragments ($Z=1$), helium projectile fragments ($Z=2$), and heavier projectile fragments (PF) with charge $Z\geqslant 3$ are denoted by n_p, n_α, and n_f, respectively.

Nuclear emulsion is a composite medium composed of hydrogen (H,$A_t=1$), light (CNO,$A_t=14$), and heavy (AgBr,$A_t=94$) nuclei. Certainly, there are also other nuclei in emulsions, but their concentrations are too small to be taken into account [14]. The separation technique, which has been used here, is based on the number n_h of target fragments. Events with $n_h=0,1$ are mainly due to ^{24}Mg-H interactions (free and quasifree nucleon) and interactions with other targets (interactions with only one bound nucleon in CNO or AgBr target nuclei). The events having $2\leqslant n_h\leqslant 7$are mostly interactions with CNO targets with some admixture of peripheral ^{24}Mg-AgBr interactions. All events with $n_h\geqslant 8$ are only due to ^{24}Mg-AgBr interactions. By following Refs. [7,29,30], this classification of the group of events with $n_h=0-1$, $2-7$, and $\geqslant 8$ can be used to elucidate the nature of the interactions with the three components H, CNO, and AgBr of target emulsion nuclei, respectively.

III. RESULTS AND DISCUSSIONS

Table I shows the event statistics for the present sample with the total projectile destruction (TD) compared with three samples given by the EMU01 Collaboration [26]. TD

TABLE II. Percentage of the total projectile destruction (TD) events in interactions of ^{24}Mg, ^{28}Si and ^{32}S projectiles with the various components of target emulsion nuclei at different energies.

Projectile	^{24}Mg		^{28}Si		^{32}Si		
Energy (*A* GeV)	3.7		3.7	14.6		200	
	Expt.%	Calc.%	Expt.%	Calc.%	Expt.%	Expt.%	Calc.%
$n_h=0,1$	18±2	16	17±2	21	18±2	18±3	18
$n_h=2-7$	42±3	47	37±3	47	40±3	35±5	43
$n_h\geqslant 8$	73±4	70	66±4	68	71±4	65±6	65
Reference	present work		[26]		[26]		

events are defined as those events where only projectile fragments with charge $Z\leqslant 2$ remain [26]. The present measured values are seen to be in systematic agreement with those obtained from other interactions. The ratio between the number of collisions having $2\leqslant n_h\leqslant 7$ (CNO and peripheral AgBr target nuclei) and the number of collisions with $n_h \geqslant 8$ (only AgBr target nuclei) is independent of the beam energy.

Based on a geometrical formula of Bradt and Peters [31] for inelastic nucleus-nucleus interactions, Adamovich *et al.* [26] have parametrized the cross section of TD events such that

$$\sigma_{TD} = (1.58A_1^{0.026})^2(A_1^{1/3} + A_2^{1/3} - 0.85A_1^{0.38})^2 \text{ fm}^2, \quad (1)$$

where A_1 and A_2 denote the mass numbers of colliding nuclei. Table II illustrates the comparison between the experimental and calculated percentages of TD events in interactions of ^{24}Mg (3.7*A* GeV), ^{28}Si (3.7*A* GeV and 14.6*A* GeV), and ^{32}S (200*A* GeV) projectiles with the targets of nuclear emulsion. The fraction of TD events for each group of target nuclei is the same within the errors at all energies and agrees well with the predictions of Eq. (1). This agreement was also observed in Refs. [26,29] for ^{28}Si (3.7*A* GeV and 14.6*A* GeV), and ^{32}S (200*A* GeV). Therefore one can conclude that the yield of total destruction of events is energy independent within the range 4–200 *A* GeV.

Table III shows that the average multiplicities of the different charged projectile fragments in interactions of ^{24}Mg projectile with different components (different ranges of n_h, i.e., H, CNO, *Em*, and AgBr nuclei) of emulsion nuclei are in a similar trend with those obtained previously for ^{22}Ne [32] and ^{28}Si [7] beam interactions with groups of emulsion nuclei at Dubna energy. The dependence of average projectile fragment numbers on the target mass is clear in the case of charge $Z\geqslant 3$. As the target mass increases, the average multiplicities of fragments $\langle n_f\rangle$ with charges $Z\geqslant 3$ decrease substantially. The mean number of helium fragments $\langle n_\alpha\rangle$ stripped in the interactions with heavy target nuclei (AgBr) is smaller than that stripped in the collisions with hydrogen target nuclei. No target mass dependence is, however, seen in the emission of fast singly charged projectile fragments.

Table IV presents the mean multiplicities of projectile fragments $\langle n_f\rangle\times 100$ with charge Z of the total sample ($n_h \geqslant 0$, i.e., *Em*) and the quasinucleon events ($n_h=0,1$, i.e., H) in interactions of 3.7*A* GeV ^{24}Mg, 3.7*A* GeV ^{28}Si [26], 14.6*A* GeV ^{28}Si [26], 200*A* GeV ^{32}S [26] with emulsion nuclei. It is clear that the average multiplicity of all fragments $\langle n_f\rangle$ is the same within statistical errors in the case of the total sample at Dubna, BNL, and SPS energies. In the quasinucleon events, if one combines all charges ($Z\geqslant 3$), the average multiplicity for these fragments is the same within errors at different projectile energies. The helium nuclei are the most frequent among the multiple charged fragments. The average multiplicity of He fragments $\langle n_\alpha\rangle$ is almost more than ten times greater than the yield of any other fragments $\langle n_f\rangle$, which suggests that the emission of these fragments does not depend on the energy of the incident nucleus. Reference. [33] has been shown that the ratio between He and H

TABLE III. The average multiplicities of the different charged (Z) projectile fragments stripped in ^{22}Ne [32], ^{24}Mg, and ^{28}Si [7] beams interactions with the various emulsion groups of nuclei at 3.7*A* GeV.

Fragment charge Z	Projectile nucleus	H	CNO	*Em*	AgBr	Ref.
1	^{22}N	1.17±0.02	1.47±0.04	1.36±0.02	1.37±0.03	[32]
	^{24}Mg	1.38±0.09	1.99±0.08	1.61±0.04	1.41±0.06	present work
	^{28}Si	1.36±0.10	1.59±0.10	1.53±0.05	1.54±0.07	[7]
2	^{22}N	1.02±0.04	0.92±0.03	0.82±0.02	0.63±0.02	[32]
	^{24}Mg	1.11±0.09	0.96±0.06	0.86±0.03	0.67±0.04	present work
	^{28}Si	1.34±0.10	1.24±0.08	1.06±0.03	0.85±0.04	[7]
⩾3	^{22}N	0.79±0.03	0.57±0.02	0.48±0.01	0.21±0.01	[32]
	^{24}Mg	0.80±0.08	0.62±0.03	0.49±0.03	0.26±0.02	present work
	^{28}Si	0.81±0.06	0.67±0.04	0.49±0.02	0.23±0.01	[7]

TABLE IV. The average multiplicities of projectile fragments $\langle n_f \rangle \times 100$ stripped in quasinucleon events (H) and in minimum-bias events (*Em*).

	$\langle n_f \rangle \times 100$							
	3.7*A* GeV				14.6*A* GeV		200*A* GeV	
Charge Z	^{24}Mg-H	^{24}Mg-*Em*	^{28}Si-H	^{28}Si-*Em*	^{28}Si-H	^{28}Si-*Em*	^{32}Si-H	^{32}Si-*Em*
2	110.9±8.8	85.9±3.4	121.0±8.0	96.0±3.0	100.0±9.0	98.0±3.0	78.0±3.0	85.0±5.0
3	2.4±1.1	3.6±0.6	3.7±0.9	4.1±0.5	2.6±1.0	3.3±0.5	2.8±1.1	3.5±0.7
4	4.7±1.5	4.4±0.7	4.6±1.1	3.8±0.2	4.0±1.4	3.7±0.4	2.8±1.1	4.0±0.7
5	5.2±1.6	6.2±0.8	4.4±1.0	4.7±0.5	5.3±1.5	4.2±0.5	2.5±1.0	3.7±0.7
6	7.6±2.0	6.2±0.8	8.8±1.5	6.1±0.6	6.0±1.5	5.4±0.5	3.5±1.1	4.8±0.8
7	9.5±2.2	6.5±0.8	8.1±1.4	6.0±0.6	4.5±1.3	5.1±0.5	4.6±1.3	4.9±0.8
8	10.4±2.3	6.3±0.8	9.0±1.5	6.1±0.6	6.0±1.5	5.5±0.5	5.3±1.4	5.5±0.9
9	8.1±2.0	4.4±0.7	7.4±1.4	5.5±0.5	7.2±1.7	5.4±0.5	7.8±1.7	5.4±0.9
10	11.4±2.5	4.5±0.7	9.5±1.6	5.4±0.5	6.0±1.5	5.7±0.5	5.3±1.4	4.9±0.8
11	11.4±2.5	4.3±0.1	6.7±1.9	4.0±0.5	7.2±1.7	4.4±0.5	6.4±1.6	4.5±0.8
12	9.5±2.2	2.7±0.5	10.4±1.6	4.5±0.5	14.7±2.5	4.1±0.5	5.9±1.4	4.3±0.7
13			6.2±1.3	3.2±0.4	9.8±2.0	3.0±0.4	7.1±1.6	3.4±0.7
14			6.5±1.3	2.3±0.3	7.5±1.7	2.5±0.3	14.5±2.4	6.3±0.9
15							12.4±2.2	5.9±0.9
16							6.0±1.5	2.6±0.6
$\geqslant 3$	80.2±8.3	49.1±2.7	85.0±6.0	56.0±2.0	82.0±7.0	53.0±3.0	86.0±7.0	64.0±4.0
Ref.	present work	present work	[26]	[26]	[26]	[26]	[26]	[26]

fragments decreases as the overlap between the colliding nuclei increases (see Table III). The cascade evaporation model [33] does not account for the existence of such α structures inside the nuclei and significantly underestimates the yield of the doubly charged fragments.

Figures 1(a)–1(d) exhibit the comparison of calculated total charge distributions of nuclear fragments (noninteracting projectile fragments) $P(Q)$ with those experimentally measured in interactions of the ^{24}Mg projectile with different components of emulsion nuclei at 3.7*A* GeV. The curves are calculated according to the Glauber extended model [34]. It can be clearly seen that Figs. 1(a)–1(d) prove good agreement between the experimental and calculated distributions. The shapes of the distributions are very different. The dependence of the total charge Q of the spectator fragments on the impact parameter (indicated by n_h) can also be noticed in Figs. 1(a)–1(d), i.e., these distributions depend strongly on the mass of the target nuclei. For the collisions with quasinucleon target (i.e., ^{24}Mg-H events) the Q distribution is peaked close to the charge Z_p of the primary, and essentially does not extend below $Z_p/2$while in the collisions with heavier targets (i.e., ^{24}Mg-AgBr events) the distribution is almost flat over the entire Q range. This behavior results in the decrease of $\langle Q \rangle$ with the increase of the target mass (see Table III). The differences in the fragmentation of the projectile nucleus on various targets are apparent. The probability of interactions without any projectile fragments with charges $Z>2$ are zero for a hydrogen target, but it increases with the increasing of the target mass. An opposite tendency is observed for events with only one fragment. All the above observations show that the disruption of the magnesium nucleus is more severe in interactions with heavy nuclei than with lighter ones.

For more comparison with the present experiment, a site percolation model [35–37] in which the nucleus is considered as a cubic lattice, [7,26] in which every lattice site represents a single nucleon and each nucleon (lattice site) has bonds to its adjacent nucleons, has been chosen. Each bond is randomly unbroken or broken. Only one parameter P called probability concentration, the probability of breaking a bond (1-P) is introduced after the dimension of the lattice is set. For the present experimental results, a simple cubic lattice is a good approximation and the calculated mass distribution is converted into a charge distribution by considering all $A=3,4$ isotopes to be $Z=2$ and $A=5,6$ isotopes to be $Z=3$, etc. Figure 2 illustrates the average charge $\langle n(Z) \rangle$ distribution of $Z \geqslant 2$ projectile fragments in ^{24}Mg interactions with the quasinucleon target ($n_h=0,1$) at 3.7*A* GeV compared with the predictions of the bond-percolation model for $P=0.55$ and $P=0.60$. These calculations are in good agreement with the measured charge distribution for $Z \geqslant 5$; also a rise in $Z=2$ is predicted. But for $Z<5$, the model prediction does not fit well the experimental data.

The critical value of P is about 0.75 [26] and hence the fit for $P \approx 0.55$ indicates that the breakup appears from subcritical systems on the average. Naturally, no kind of pre-formed α substructures is introduced in the percolation simulation, which may be the reason for the underestimation of the He yield [26].

Figure 3 shows the multiplicity distributions of $Z \geqslant 2$ fragments in the present ^{24}Mg and ^{28}Si [26] incident beams on the quasinucleon (H-target) type compared to the calculations of the bond percolation approach with $P=0.55$ and $P=0.60$. It is seen that the model predictions are in satisfactory agreement with the experimental data.

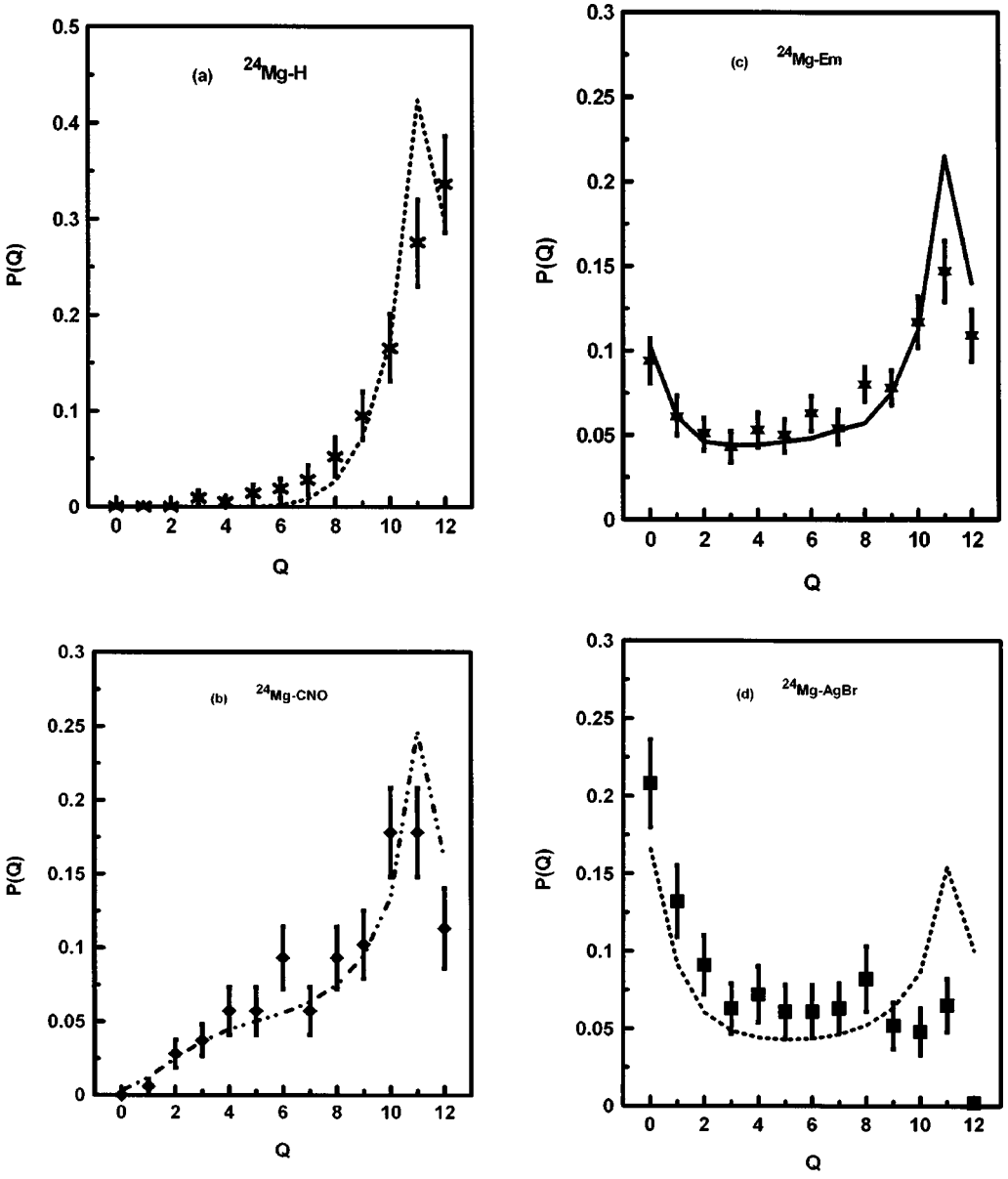

FIG. 1. (a)–(d) The experimental (points with error bars) and calculated (curves) total charge distributions of nuclear fragments stripped in the interactions of 3.7*A* GeV ^{24}Mg projectile with: (a) H, free and quasifree nucleon type ($n_h=0,1$), (b) CNO type ($2\leqslant n_h\leqslant 7$), (c) *Em* nuclei ($n_h\geqslant 0$), and (d) AgBr type ($n_h\geqslant 8$). The curves are the predictions of the extended Glauber model.

To know about the degree of "peripherality" and/or "centrality" of an event, the information about the impact parameter (b) between the centers of two colliding nuclei is necessary from the geometrical point of view. This parameter determines the number of interacting nucleons from both projectile and target nuclei. It is an unobserved physical quantity and if a certain degree of precision in the experimental analysis is sought, then an observable measurable quantity should be chosen as a measure for this parameter. The experimental qualitative measure is usually chosen to be either the total charge of the projectile spectators Q or the heavy-ionizing-particle multiplicity n_h (which is a target size parameter) or both. The number of interacting projectile nucleons N_{int} can be estimated event-by-event from the following formula:

$$N_{int} = A_p - \left(\frac{A_p}{Z_p}\right)Q, \tag{2}$$

where A_p (Z_p) is the mass (charge) number of the projectile nucleus. The dependence of the average number of interacting projectile nucleons $\langle N_{int}\rangle$ on the degrees of disintegration of the target nuclei (collision geometry, i.e., different impact parameter) in ^{24}Mg-*Em* interactions is represented in Fig. 4. This figure indicates that even in collisions where no or very little excitation of target occurs (i.e., $n_h=0,1$), some of the projectile nucleons take part in the interaction. As expected, the average number of interacting projectile nucleons increases substantially as n_h increases from peripheral to central collisions but attains a more or less constant value for extreme central collisions. The average highest value of

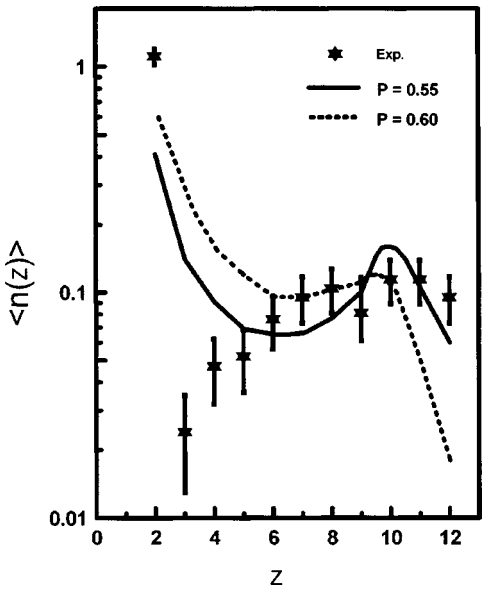

FIG. 2. Charge distributions of nuclear projectile fragments emerged in ^{24}Mg interactions with quasinucleon target ($n_h=0,1$) at 3.7*A* GeV. The curves are calculated by the bond percolation model with parameters $P=0.55$ and 0.60.

$\langle N_{int}\rangle$ in this experiment is 22.85 ± 0.83, implying the participation of nearly 95% of projectile nucleons in the collision process. These events, representing almost 5% of the total sample, are examples of extreme central collisions where it is expected that almost all nucleons of the projectile and the majority nucleons of the heavy AgBr target nuclei take part in the collision [7,38,39]. These events are potentially useful for seeking evidence for the formation of quark-gluon plasma.

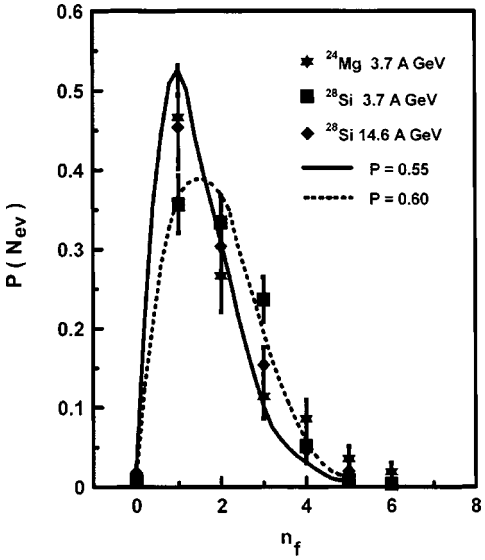

FIG. 3. The multiplicity distributions of projectile fragments with charge $Z\geq2$ in interactions of 3.7*A* GeV ^{24}Mg, 3.7*A* GeV ^{28}Si [26], and 14.6*A* GeV ^{28}Si [26] incident beams on the quasinucleon target. The curves are calculated according to the percolation model.

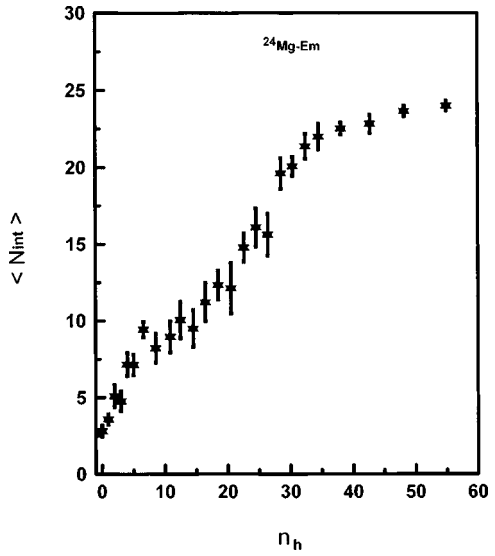

FIG. 4. The relation between the average number of interacting projectile nucleons $\langle N_{int}\rangle$ and the number of heavily target fragments n_h in ^{24}Mg*Em* interactions at 3.7*A* GeV.

The topology summarized in Table V for the nuclear fragmentation modes of the visible channels in incident ^{24}Mg projectile on the different components of emulsion nuclei at 3.7*A* GeV compared with those yield in ^{28}Si (3.7*A* GeV and 14.6*A* GeV) and ^{32}S (200*A* GeV) beams interactions with the same targets of emulsion nuclei [26]. Some or all H fragments represent the participant nucleons, so that the sum of charges of all projectile fragments in each channel must be Z_p. The fractions of the present sample, within the statistical errors, are very close to those obtained previously for different projectiles at different energies [26]. After a keen examination of Table V, the following points can be drawn:

(i) The relative rates of nuclear fragmentation channels from the incident nuclei are almost the same fraction for all projectiles at different energies, revealing that the modes of nuclear fragmentation are energy independent.

(ii) The stripped processes with relativistic hydrogen and/or helium fragments are the dominant in all projectiles.

(iii) The majority of the multiple charged fragments are helium nuclei and yields are up to $n_\alpha=(Z_p-2)/2$. The channels in which several heavy fragments ($Z_{max}\geqslant3$) are stripped from the projectile nuclei are also accompanied by several alpha particles. The fractional yield of nuclear fragmentation channels without any projectile fragments heavier than helium fragments (channels that having only fragments with $Z_{max}\leqslant2$ and $n_f=0$) is about 27% of the total sample and the most frequent in these channels are those with one alpha fragment which represents almost 10% for all projectiles.

(iv) There are considerable numbers of interactions in which the projectile nuclei break up into single charged particles only (the channels having only the fast moving hydrogen fragments with $Z_{max}=1$ and $n_\alpha=n_f=0$). These interactions represent $\approx14\%$ of all the analyzed events and are mostly due to central collisions in which the majority of projectile nucleons have participated in the first stage of the collisions, i.e., in the process of particle production [1].

(v) The disruptive heavy projectile fragments that have

TABLE V. Topology of the present 3.7*A* GeV ^{24}Mg nuclear fragmentation is compared with those obtained in ^{28}Si and ^{32}S incident projectiles on emulsion nuclei at 3.7, 14.6*A* GeV and 200*A* GeV [26].

Projectile	Channels	n_h				Fraction (%) of total sample	Reference
		0–1	2–7	⩾8	⩾0		
^{24}Mg at 3.7*A* GeV	Mg	20	8		28	2.73±0.52	present work
	Na+H	24	19	1	44	4.29±0.66	
	Ne+He	5	1		6	4.49±0.68	
	Ne+2H	19	15	6	40		
	F+He+H	8	2		10	4.39±0.67	
	F+3H	9	20	6	35		
	O+Be			1	1	6.34±0.81	
	O+2He	6	2		8		
	O+He+2H	11	14	6	31		
	O+4H	5	12	8	25		
	N+B		1		1	6.54±0.82	
	N+Be+H			1	1		
	N+2He+H	5	2	1	8		
	N+He+3H	12	19	1	32		
	N+5H	3	16	6	25		
	C+Li+He+H		1		1	6.15±0.80	
	C+Li+3H	1			1		
	C+3He	1			1		
	C+2He+2H	2	2	4	8		
	C+He+4H	8	14	8	30		
	C+6H	4	7	11	22		
	B+Be+He+H	1			1	6.24±0.80	
	2B+2H			1	1		
	B+3He+H	2	2		4		
	B+2He+3H	3	6	2	11		
	B+He+5H	4	13	12	29		
	B+7H	1	12	5	18		
	2Be+He+2H		1		1	4.29±0.66	
	2Be+4H	1			1		
	Be+Li+He+3H	1			1		
	Be+3He+2H	1			1		
	Be+2He+4H	4	3	1	8		
	Be+He+6H	3	4	11	18		
	Be+8H		5	9	14		
	Li+3He+3H	1		1	2	3.61±0.60	
	Li+2He+5H	2	4	4	10		
	Li+He+7H	1	6	9	16		
	Li+9H	1	5	3	9		
	5He+2H	4	4	2	10	27.41±1.85	
	4He+4H	9	14	5	28		
	3He+6H	13	12	13	38		
	2He+8H	9	37	51	97		
	He+10H	4	38	66	108		
	12H	3	34	112	149	14.54±1.27	
	O[a]		9	83	92	8.98±0.98	
	all	211	364	450	1025		
^{28}Si at 3.7*A* GeV	Si	28	13	6	47	2.38±0.35	[26]

TABLE V. (*Continued*.)

Projectile	Channels	n_h				Fraction (%) of total sample	Reference
	Al+H	27	37	6	70	3.54±0.43	
	Mg+He	16	4		20	4.46±0.49	
	Mg+2H	29	34	5	68		
	Na+He+H	15	10		25	4.05±0.46	
	Na+3H	14	24	17	55		
	Ne+2He	8	2	1	11	5.52±0.54	
	Ne+He+H	16	18	6	40		
	Ne+4H	17	27	14	58		
	F+2He+H	7	10	1	18	5.67±0.55	
	F+He+3H	13	16	10	39		
	F+5H	12	29	14	55		
	O+C	1			1	6.08±0.57	
	O+Be+2H	1			1		
	O+3He	2	3	1	6		
	O+2He+2H	12	7	2	21		
	O+He+4H	18	24	10	52		
	O+6H	5	22	12	39		
	N+C		1		1	5.87±0.56	
	N+B+H		3		3		
	N+3He+H	1	3	2	6		
	N+2He+3H	11	15	4	30		
	N+He+5H	19	17	9	45		
	N+7H	4	11	16	31		
	2C+2H	1		1	2	5.87±0.56	
	C+B+2He	1			1		
	C+B+He+H	1	2		3		
	C+B+3H	1			1		
	C+Be+4H			1	1		
	C+Li+He+3H	1	1	1	3		
	C+Li+5H		1		1		
	C+3He+2H	3	3	1	7		
	C+2He+4H	18	16	6	40		
	C+He+6H	8	14	13	35		
	C+8H	2	12	8	22		
	B+Be+He+3H		1		1	4.30±0.48	
	B+Be+5H	1	1		2		
	B+Li+He+4H	2			2		
	B+Li+6H		2		2		
	B+3He+3H	3	5		8		
	B+2He+5H	4	11	5	20		
	B+He+7H	4	18	10	32		
	B+9H	2	7	9	18		
	2Be+He+4H			1	1	3.34±0.42	
	2Be+6H			1	1		
	Be+Li+He+5H		1		1		
	Be+4He+2H	1			1		
	Be+3He+4H	2	1	2	5		
	Be+2He+6H	6	5	3	14		

TABLE V. (*Continued.*)

Projectile	Channels	n_h				Fraction (%) of total sample	Reference
	Be+He+8H	6	8	9	23		
	Be+10H	3	7	10	20		
	2Li+He+6H		2	2	4	3.49±0.43	
	2Li+8H	1	1		2		
	Li+5He+H		1		1		
	Li+4He+3H			2	2		
	Li+3He+5H	2	1	2	5		
	Li+2He+7H	5	5	6	16		
	Li+He+9H	3	6	11	20		
	Li+11H	1	6	12	19		
	6He+2H	5	1		6	27.75±1.34	
	5He+4H	4	6	3	13		
	4He+6H	11	27	8	46		
	3He+8H	26	45	51	122		
	2He+10H	16	59	78	153		
	He+12H	10	66	132	208		
	14H	3	60	227	290	14.68±0.92	
	O[a]		1	58	59	2.99±0.39	
	all	433	733	809	1975		
^{28}Si at 14.6*A* GeV	Si	20	7		27	2.83±0.55	[26]
	Al+H	26	15	1	42	4.40±0.69	
	Mg+He	8			8	6.07±0.82	
	Mg+2H	31	15	4	50		
	Na+He+H	7	2		9	4.29±0.65	
	Na+3H	12	18	2	32		
	Ne+2He	1	1		2	4.19±0.68	
	Ne+He+H	9	8	2	19		
	Ne+4H	6	11	2	19		
	F+2He+H	3	2	1	6	3.98±0.66	
	F+He+3H	9	7	3	19		
	F+5H	6	4	3	13		
	O+3He	1		1	2	5.55±0.78	
	O+2He+2H	4	3	1	8		
	O+He+4H	6	11	6	23		
	O+6H	5	8	7	20		
	N+Be+2H		1		1	5.65±0.79	
	N+Li+4H	1	1		2		
	N+3He+H	1	1		2		
	N+2He+3H	3	5	3	11		
	N+He+5H	7	10	8	25		
	N+7H		7	6	13		
	2C+2H	1			1	6.18±0.83	
	C+Be+He+2H	1			1		
	C+Li+5H	1			1		
	C+3He+2H	1	1		2		
	C+2He+4H	5	7	6	18		
	C+He+6H	5	6	7	18		
	C+8H	3	6	9	18		

TABLE V. (*Continued.*)

Projectile	Channels	n_h				Fraction (%) of total sample	Reference
	B+Be+He+3H	1			1	4.29±0.65	
	B+2Li+3H		1		1		
	B+3He+3H	1		1	2		
	B+2He+5H	2	8	1	11		
	B+He+7H	9	8	5	22		
	B+9H	1	2	1	4		
	2Be+He+4H	1		1	2	3.77±0.64	
	2Be+6H			1	1		
	Be+Li+He+5H	1			1		
	Be+5He		1		1		
	Be+3He+4H	3	2		5		
	Be+2He+6H	3	1		4		
	Be+He+8H	1	6	6	13		
	Be+10H	1	7	1	9		
	Li+4He+3H		2		2	3.14±0.58	
	Li+3He+5H	1		2	3		
	Li+2He+7H	3	5	1	9		
	Li+He+9H	1	5	3	9		
	Li+11H		3	4	7		
	6He+2H		1		1	26.49±1.87	
	5He+4H	6	6	2	14		
	4He+6H	4	7	9	20		
	3He+8H	13	23	14	50		
	2He+10H	16	19	34	69		
	He+12H	8	31	60	99		
	14H	5	32	103	140	14.66±1.33	
	O[a]	1	1	41	43	4.50±0.70	
	all	265	328	362	955		
^{32}S at 200*A* GeV	S	17	3		20	2.58±0.58	[26]
	P+H	35	10	1	46	5.94±0.90	
	Si+He	14			14	6.32±0.93	
	Si+2H	27	6	2	35		
	Al+He+H		1		1	3.35±0.67	
	Al+3H	17	6	2	25		
	Mg+Li+H	1			1	4.39±0.77	
	Mg+2He	2	1		3		
	Mg+He+2H	1	1	2	4		
	Mg+4H	11	11	4	26		
	Na+He+3H	2		3	5	4.52±0.78	
	Na+5H	16	9	5	30		
	Ne+2He+2H		1	1	2	4.90±0.81	
	Ne+He+4H	4	4	2	10		
	Ne+6H	11	11	4	26		
	F+3He+H	1			1	5.42±0.86	
	F+2He+3H	1	1		2		
	F+He+5H	9	3	1	13		
	F+7H	11	9	6	26		
	O+3He+2H	2	1		3	5.55±0.87	

TABLE V. (*Continued.*)

Projectile	Channels	n_h				Fraction (%) of total sample	Reference
	O+2He+4H	1	2		3		
	O+He+6H	7	9	3	19		
	O+8H	5	7	6	18		
	N+Be+He+3H		1		1	4.90±0.81	
	N+Li+He+4H	1			1		
	N+4He+H	3			3		
	N+3He+3H		2	1	3		
	N+2He+5H	3	1	1	5		
	N+He+7H	5	5	6	16		
	N+9H	1	3	5	9		
	2C+He+2H		1		1	4.65±0.79	
	C+Be+He+4H			1	1		
	C+Be+6H	1			1		
	C+Li+He+5H	1			1		
	C+3He+4H	1			1		
	C+2He+6H	3	6	2	11		
	C+He+8H	2	8	2	12		
	C+10H	2	3	3	8		
	2B+He+4H		1		1	3.35±0.67	
	2B+6H	1	1		2		
	B+Be+2He+3H	1			1		
	B+Be+He+5H		1		1		
	B+Li+He+6H		1		1		
	B+3He+5H		1	1	2		
	B+2He+7H	2	3	2	7		
	B+He+9H	1	1	2	4		
	B+11H	1	6		7		
	2Be+He+6H			1	1	3.35±0.67	
	2Be+8H			1	1		
	Be+Li+2He+5H			1	1		
	Be+Li+He+7H		1		1		
	Be+3He+6H	1	1	1	3		
	Be+2He+8H	2	1	5	8		
	Be+He+10H	2		3	5		
	Be+12H		2	4	6		
	2Li+He+8H	1			1	2.58±0.58	
	Li+2He+9H	1	4	2	7		
	Li+He+11H	1	4	3	8		
	Li+13H	1		3	4		
	7He+2H	1			1	22.19±1.87	
	6He+4H			1	1		
	5He+6H	7	1	1	9		
	4He+8H	6	10	3	19		
	3He+10H	8	12	8	28		
	2He+12H	6	27	22	55		
	He+14H	7	17	35	59		
	O[a]	15	13	96	124	16.00±1.55	
	all	283	234	258	775		

[a]No fragmentation inside the forward cone.

$Z_{max} \geq 9$ (channels of P, Si, Al, Mg, Na, Ne, and F stripped nuclei having average binding energy per nucleon $\langle E_B \rangle$ are greater than 8 MeV) associated with the hydrogen fragments are mostly abundant while their disruption accompanied by the helium fragments are the next one at all energies.

(vi) For all systems, the yields of relativistic He fragments accompanied by one of the projectile fragments having maximum charges in the range of $3 \leq Z_{max} \leq 8$ (channels of O, N, C, B, Be, and Li fragmented nuclei that have $\langle E_B \rangle < 8$ MeV) are more of a contribution than the fragmentation of these nuclei associated with H fragments only.

(vii) The least percentage for the nuclear fragmentation processes is 2.5% in the case of the emerged single heavier fragment and has the same charge of the incident projectile ($Z_{max} = Z_p$) for all beams. These channels are mostly due to the elastic scattering events, high energy δ rays and low energy $e^+ e^-$ pairs [28].

(viii) The nuclear fragmentation processes of the incident projectile into two stripped nuclei or double fragmented nuclei are rare at all energies. For example, the channels of the ^{24}Mg projectile fragmented into once: for O+Be, N+B, N+Be, C+Li, 2B, and 2Be stripped nuclei represents 0.6% of the total sample. It can be noted that there is no significant evidence for binary fission produced enhancement in the $3 \leq Z_{max} \leq 8$ region in these channels, such as that seen at lower energies with the ^{197}Au projectile [9]. The authors of Refs. [9,14] have reported a similar result in interactions of gold nuclei with emulsion targets at 10.6*A* GeV energies.

(xi) As expected, the stripped heavier projectile fragments are the most abundant in the interactions with the light target nuclei (H, CNO; the gentle low excitation energy processes) while the lighter projectile fragments emerged enhancement in the interactions with the heavy target nuclei (AgBr; the violent high excitation energy processes), indicating the role of the impact parameter collision in the fragmentation mechanism.

(x) For a hydrogen target there are no events with $n_f = 0$, while 80% of events have only one fragment with $Z_{max} > 2$. For heavier targets (AgBr), the fraction of events with $n_f = 0$ increases with increasing target mass. Also the number of released protons and helium fragments from ^{24}Mg, ^{28}Si, and ^{32}S projectiles in interactions with heavy nuclei is three times and twice as large as in interactions with light nuclei, respectively. Again, these facts lead to the conclusion that the disruption of the residual projectile nuclei is more pronounced in interactions with heavy nuclei than with light ones. The same result has been reported previously in interactions of 10.6*A* GeV gold nuclei with light and heavy target nuclei in nuclear emulsion [10].

IV. CONCLUSIONS

The nuclear fragmentation properties in interactions of a 3.7*A* GeV ^{24}Mg projectile with the different nuclei of nuclear emulsion are investigated. These results have been compared with the present calculations that are based on the extended Glauber model and percolation approach as well as the other experimental data. After this study we reach the following important conclusions:

The experimental cross sections of total projectile destruction events are reproduced by the geometrical formula of Bradt and Peters. The charge, size, and multiplicity distributions of projectile fragments are nearly the same in energy ranged from 3.7 to 200*A* GeV. Thus the limiting fragmentation hypothesis is achieved in the nuclear processes of the projectile fragmentations.

The total charge distributions of nuclear fragments are well described by the predictions of the extended Glauber model. For quasinucleon target events, the size of the fragmenting system is well defined; the multiplicity and charge distributions of fragments with $Z \geq 5$ are found to agree well with the calculations of the bond percolation model. Also the single parameter P of this model is sensitive to the distributions of fragments.

The fragmentation of the projectile magnesium nucleus depends strongly on the target mass. This is manifested in different average multiplicities of the charged Z of fragments and the distributions of the total charge Q confined in multiple charged projectile fragments. In the lighter target nucleus, the more frequent are heavier projectile fragments and the larger mean values of the total charge confined in multiple charged projectile fragments.

The magnesium projectile nucleus is bigger than the light target nuclei (H, CNO); all interactions with hydrogen target and the majority of interactions with light nuclei (CNO) are peripheral. Only for ^{24}Mg interactions with heavy target nuclei (AgBr) the number of intranuclear collisions is large, leading to events with small charge Z of the heaviest fragment of the projectile and also a small total charge Q emerged forward, showing a greater degree of breakup of the projectile nucleus by the heavy targets.

The relative rates of nuclear fragmentation channels from incident nuclei are almost the same fraction for all projectiles at different energies, revealing that the modes of nuclear fragmentation are energy independent. The stripped processes with relativistic hydrogen and/or helium fragments are dominant in all projectiles. The majority of the multiple charged fragments are helium nuclei and the fragmentation channels in which several heavy fragments ($Z_{max} \geq 3$) are stripped from the projectile nuclei are also accompanied by several alpha particles. The fractional yield of nuclear fragmentation channels without projectile fragments that are heavier than helium fragments is about 27% of the total sample and the most frequent in these channels are those with one alpha fragment and represents almost 10% for all projectiles. The interactions in which the projectile nuclei break up into single charged particles represent $\approx$14% of the total sample and are mostly due to central collisions in which the majority of projectile nucleons have participated in the first stage of the collisions, i.e., in the process of particle production.

The disruptive nuclei that have $\langle E_B \rangle > 8$ MeV are mostly stripped associated with the hydrogen fragments while the fragmented nuclei having $\langle E_B \rangle < 8$ MeV are tendency emerged accompanied with helium fragments. It is interesting to note that this data set for ^{24}Mg, ^{28}Si, and ^{32}S does not give any evidence of the occurrence of binary fission in the charge range of $3 \leq Z_{max} \leq 8$.

The stripped heavier projectile fragments are the most abundant from the interactions with the light target nuclei (the gentle low-temperature processes) while the lighter projectile fragments emerged enhancement in the interactions with the heavy target nuclei (the violent high-temperature processes); indicating the role of the impact parameter collision in the fragmentation mechanism. For a hydrogen target there are no events with $n_f=0$, while 80% of events have only one fragment with $Z_{\max}>2$. For heavier targets (AgBr), the fraction of events with $n_f=0$ increases with increasing target mass. The disruption of the residual projectile nuclei is more pronounced in interactions with heavy nuclei than with light ones. The fragmentation of the nuclei undergoing these energetic interactions may proceed through the creation of a residual excited nucleus and then a slow deexcitation, which proceeds by consecutive emission of nuclear fragments.

[1] M. A. Jilany, J. Phys. G **29**, 2263 (2003), and references therein.
[2] Fu-hu Liu and Yuri A. Panebratsev, Phys. Rev. C **59**, 941 (1999), and references therein.
[3] Fu-hu Liu and Yuri A. Panebratsev, Nuovo Cimento Soc. Ital. Fis., A **111**, 1219 (1998).
[4] J. Hüfner, Phys. Rep. **125**, 129 (1985).
[5] J. D. Bowman, Lawrence Berkeley Laboratory Report No. LBL 2908 1973; J. Hüfner, Report No. GSI 80-1, 1980.
[6] H. R. Schmidt and J. Schukraft, Report No. CERN-PPE/92-42 1992.
[7] B. K. Singh and S. K. Tuli, Nuovo Cimento Soc. Ital. Fis., A **112**, 1093 (1999).
[8] M. L. Cherry *et al.*, Acta Phys. Pol. B **29**, 2155 (1998).
[9] M. L. Cherry *et al.*, Phys. Rev. C **52**, 2652 (1995).
[10] M. L. Cherry *et al.*, Z. Phys. C **63**, 549 (1994).
[11] A. Ferrari *et al.*, Z. Phys. C **71**, 75 (1996).
[12] B. Wilczynska *et al.*, 26th International Cosmic Ray Conference, Salt Lake City, Utah, 1999.
[13] C. J. Waddington and P. S. Freier, Phys. Rev. C **31**, 888 (1985).
[14] M. I. Adamovich *et al.*, Eur. Phys. J. A **5**, 429 (1999), and references therein.
[15] M. L. Cherry *et al.*, Eur. Phys. J. C **5**, 641 (1998).
[16] G. Singh and P. L. Jain, Phys. Rev. C **54**, 3185 (1996).
[17] W. A. Friedman, Phys. Rev. C **42**, 667 (1990).
[18] R. J. Charity *et al.*, Nucl. Phys. **A483**, 371 (1988).
[19] D. H. E. Gross, Rep. Prog. Phys. **53**, 605 (1990); H. R. Jaqaman and D. H. E. Gross, Nucl. Phys. **A524**, 321 (1991).
[20] J. Bondorf *et al.*, Nucl. Phys. **A444**, 460 (1985).
[21] W. Bauer, Phys. Rev. C **38**, 1297 (1988); W. Bauer *et al.*, Annu. Rev. Nucl. Sci. **42**, 77 (1992); Nucl. Phys. **A152**, 600 (1986); J. D. Desbois, *ibid.* **A466**, 724 (1987).
[22] D. Stauffer, Phys. Rep. **54**, 1 (1979); X. Campi, Phys. Lett. B **208**, 351 (1988); J. Phys. (France) **19**, 917 (1986); X. Campi and H. Krivine, Z. Phys. A **344**, 81 (1992).
[23] X. Campi, J. Phys. A **19**, L917 (1986).
[24] EOS Collaboration, J. B. Elliott *et al.*, Phys. Lett. B **381**, 24 (1996); **418**, 35 (1998); Phys. Rev. C **62**, 064603 (2000); Phys. Rev. Lett. **85**, 1194 (2000).
[25] EOS Collaboration, J. A. Hauger *et al.*, Phys. Rev. Lett. **77**, 235 (1996); Phys. Rev. C **57**, 764 (1998).
[26] M. I. Adamovich *et al.*, Z. Phys. A **351**, 311 (1995).
[27] M. A. Jilany, Nucl. Phys. **A579**, 627 (1994).
[28] M. A. Jilany, Nucl. Phys. **A705**, 477 (2002), and references therein.
[29] M. El-Nadi, M. S. El-Nagdy, N. Ali-Mossa, A. Abdelsalam, A. M. Abdalla, and A. A. Hamed, J. Phys. G **25**, 1169 (1999).
[30] M. L. Cherry *et al.*, Eur. Phys. J. C **5**, 641 (1998).
[31] H. L. Bradt and B. Peters, Phys. Rev. **77**, 54 (1950).
[32] N. P. Andreeva *et al.*, Sov. J. Nucl. Phys. **47**, 102 (1988).
[33] A. El-Naghy *et al.*, Nucl. Phys. **14**, 1125 (1988).
[34] M. K. Hegab, M. T. Hussein, and N. M. Hassan, Z. Phys. A **336**, 345 (1990), and references therein.
[35] D. Stauffer and A. Aharony, *Introduction to Percolation Theory* (Taylor & Francis, London, 1994).
[36] H. G. Ballesteros, L. A. Fernández, V. Martín-Mayor, A. Muñoz Sudupe, G. Parisi, and J. J. Ruiz-Lorenzo, Phys. Lett. B **400**, 346 (1997); J. Phys. A **32**, 1 (1999), and references therein.
[37] Santo Fortunato, Phys. Rev. B **66**, 054107 (2002).
[38] B. K. Singh and S. K. Tuli, Nucl. Phys. **A602**, 487 (1996).
[39] M. M. Sherif, M. A. Jilany, M. N. Yasin, and S. M. Abd-Elhalim, Phys. Scr. **51**, 431 (1995).